

Morphology and thermal characterization of nanographene platelets

J. H. Koo · S. C. Lao · J. Lee · D. Z. Chen ·
C. Lam · W. Yong · M. Londa · L. A. Pilato

Received: 10 October 2010 / Accepted: 12 January 2011 / Published online: 1 February 2011
© Springer Science+Business Media, LLC 2011

Abstract This study summarizes our current research in using different types of nanographene platelets (NGPs) to create polymer–graphene nanocomposites for selective laser sintering manufacturing application. This article describes five NGPs that were available to our research group. Morphological characterization of their microstructures was examined using scanning electron microscopy. Thermal characterization of these NGPs was conducted using thermogravimetric analysis. Kinetics of these NGPs was calculated using the isoconversion technique. Similarities and differences of these NGPs were drawn from the above measurements and calculations. Two NGPs were selected for further studies.

List of symbols

A	Pre-exponential factor
A_{avg}	Average pre-exponential factor
A_s	Maximum mass loss attainable
Cpm	°C/min
E	Activation energy
E_{avg}	Average activation energy

J. H. Koo (✉) · S. C. Lao
Department of Mechanical Engineering, Texas Materials Institute, The University of Texas at Austin, Austin, TX 78712-0292, USA
e-mail: jkoo@mail.utexas.edu

J. Lee
Agency for Defense Development, Daejeon City, South Korea

D. Z. Chen · C. Lam · W. Yong · M. Londa
Department of Mechanical Engineering, The University of Texas at Austin, Austin, TX 78712-0292, USA

L. A. Pilato
KAI, LLC, Austin, TX 78739, USA

E_{peak}	Peak activation energy
k	Kinetic constant
n	Order of reaction
R	Universal gas constant
T	Temperature
t	Time
w	Instantaneous weight
X_s	Solid conversion
B	Heating rate

Subscripts

avg	Average
f	Final
o	Initial
peak	Peak

Introduction

The introduction of inorganic nanomaterials as additives into polymer matrix systems has resulted in polymer nanocomposites (PNCs) exhibiting multi-functional, high performance polymer characteristics beyond what traditional polymer composites possess [1–6]. Multi-functional features attributable to PNCs consist of improved thermal resistance, flame resistance, moisture resistance, decreased permeability, charge dissipation, and chemical resistance [1–6]. Through control/adjustment of the additive at the nanoscale level, one is able to maximize property enhancement of selected polymer systems to meet or exceed the requirements of current military, aerospace, and commercial applications.

The nanographene platelet (NGP) is an emerging class of nanomaterials. An NGP is a nanoscale platelet composed of one or more layers of a graphene plane, with a platelet thickness from 0.34 to 100 nm [7]. NGPs are predicted to have a range of unusual physical, chemical, mechanical,

and flammability properties. Although practical electronic devices for graphene are not envisioned to occur within the next 5–10 years, its application as nanofiller in a composite is imminent. The availability of processable graphene sheets in large quantities is essential to the success in exploiting composites and other applications.

The objective of this study is to summarize our current research in using different types of NGPs to create polyamide–graphene nanocomposites for selective laser sintering manufacturing application. It is an extension of our PNCs research program to include NGPs as a new type of nanomaterials [8, 9] to enhance polyamide properties. This article describes five NGPs that were available to our research group from different sources. Morphological characterization of their microstructures was examined using scanning electron microscopy (SEM). Thermal characterization of these NGPs was conducted using thermogravimetric analysis (TGA). Kinetics of these NGPs was calculated using isoconversion method.

Material systems

Nanographene platelet

Five types of nanoscale graphene platelets were obtained by our research group. Before we start using them in our PNC research we examined the morphology, thermal stability, and activation energy of each NGP. A brief description of each NGP is included in this session.

NGP-1 is provided to us by Professor Antonio F. Ávila of Universidade Federal de Minas Gerais [10]. This NGP-1 is a Brazilian product (Grafmax HC 11-IQ) manufactured by Nacional Grafite in Brazil. Ávila used this product in his hybrid nanocomposites studies [11]. Thermal stability was greatly improved when 3 wt% of NGP-1 was incorporated in an epoxy resin.

NGP-2 is a product from Graftech International (TG679). Miller used a functionalized TG679 in her studies in epoxy [12]. The functionalized TG679 NGP when added to epoxy resin produced mixed results in terms of mechanical properties enhancement. The study concluded the degree of functionalization affects the processing and properties and should be a prerequisite to designing a polymer–graphite nanocomposite.

NGP-3 is provided to us by Dr. Howard K. Schmidt of Rice University [13]. Dr. Schmidt obtained large quantities of this NGP-3 from a Russian source. No technical information is available of this material.

NGP-4 is manufactured by XG Sciences, Inc. at East Lansing, MI [14]. Their products are based on exfoliated graphite nanoplatelets. The brand name is xGnPTM, they are

Table 1 Typical properties of XGnP

Property	Values
Density	~2.0 g/cc
Chemical composition	Graphene
Electrical resistivity	~50 × 10 ⁻⁶ Ω cm
Thermal conductivity	3,000 W/m K
Tensile modulus	~1.0 GPa
Tensile strength	~10–20 GPa

small stacks of graphene sheets made through their proprietary manufacturing process. These platelets can be produced in sizes ranging from 5 to 25+ μm in diameters and with various surface treatments. It was supplied to us as a dry powder. Besides marketing their xGnP NGP, they also supply most common polymers in masterbatch formulations. Table 1 shows some typical physical, thermal, and mechanical properties of the xGnP material.

NGP-5 is a graphite oxide (GO) provided to us by Professor Rod Ruoff of the University of Texas at Austin [15]. Abundant technical information can be found in Professor Ruoff's website [15].

Polyamides

Polymerized amides joined by peptide bonds are thermoplastics noted for their relatively high-tensile strength, good creep resistance, as well as excellent abrasion, chemical, and heat resistance. The melting points for polyamide 11 (PA11) and polyamide 12 (PA12) are 183–190 and 174–180 °C, respectively. Injection molding, extrusion, blown-film extrusion, extrusion-blown molding, rotomolding, and selective laser sintering can process both PA11 and PA12. Rilsan® PA11 (Arkema Inc.) [16] and Vestamid® PA12 (Evonik) [17], both supplied in pellet form, were used in our PNC research.

Experimental and numerical

Morphology and thermal characterization

Morphological analyses were performed on all NGPs using scanning electron microscopy (SEM) at different magnifications to compare the microstructures of each NGP. The Zeiss LEO 1530 Gemini scanning electron microscope was used. Thermal characterization of these NGPs was conducted using thermogravimetric analysis (TGA) at three heating rates: 5, 20, and 40 °C/min in an argon (Ar) atmosphere. The TA Instruments SDT AQ600 was used in this study.

Kinetic parameters and the isoconversion method

The rate of thermal decomposition of polymers can be modeled by the kinetic rate equation:

$$-\frac{1}{w_0} \frac{dw}{dt} = Af \left(\frac{w}{w_0} \right)^n \exp \left(-\frac{E}{RT} \right), \quad (1)$$

where A is the pre-exponential factor, E is the activation energy, n is the order of reaction, and $f(w/w_0)$ is an arbitrary function of instantaneous weight fraction. To predict the thermal response of a polymer, accurate values of these kinetic parameters over the range of decomposition are required in a thermal model. TGA is a common polymer characterization technique to determine the thermal stability of a sample polymer by recording the weight change of the polymer as a function of increasing temperature or time at a constant rate. A furnace heats the sample while a sensitive microbalance monitors loss or gain of sample weight due to chemical reactions, decomposition, solvent or water evaporation, and oxidation. Normally, the measurement is carried out in air or in an inert environment, such as nitrogen or argon, at a constant purging rate. The multiple heating rate technique will provide the pre-exponential factor, activation energy, and order of reaction over a wide range of heating rates.

The isoconversion method is widely used to describe kinetics parameters [18]. The basic idea of the method can be summarized as follows. The rate of degradation is a function of temperature and solid conversion, X_s ,

$$\frac{dX_s}{dt} = f(T, X_s) = k(A_s - X_s)^n, \quad (2)$$

where X_s is defined as

$$X_s = \frac{w_0 - w}{w_0 - w_f}, \quad (3)$$

A_s is the maximum weight loss attainable at each temperature (value has been taken as 1.0), and k is the kinetic constant, which corresponds to the Arrhenius equation:

$$k = A \exp \left(-\frac{E}{RT} \right). \quad (4)$$

A single-order reaction is used ($n = 1$), and the Ozawa–Flynn–Wall method [19] is considered, for obtaining the value of activation energy:

$$\ln \beta = \ln \left(\frac{AE}{R} \right) - 5.33 - \ln(1 - X_s) - 1.05 \frac{E}{RT}, \quad (5)$$

where β is heating rate. Plotting $\ln \beta$ as a function of $1/T$, linear equations may be used to fit for each parametric value of X_s to obtain the values of activation energy and pre-exponential factor. These kinetic parameters imply that the thermal decomposition of the polymer can be expressed by a simple

kinetic equation, with single effective values of A and E . By adjusting the order of reaction, a separate set of kinetic parameters can be obtained, but when plotting $\log A$ as function of E , a linear curve fit can be observed using different values of n , which is the result of the kinetic compensation effect.

Results and discussion

Morphological characterization

Several magnifications of the NGPs were conducted using SEM to study their microstructures. Figure 1a–c shows the

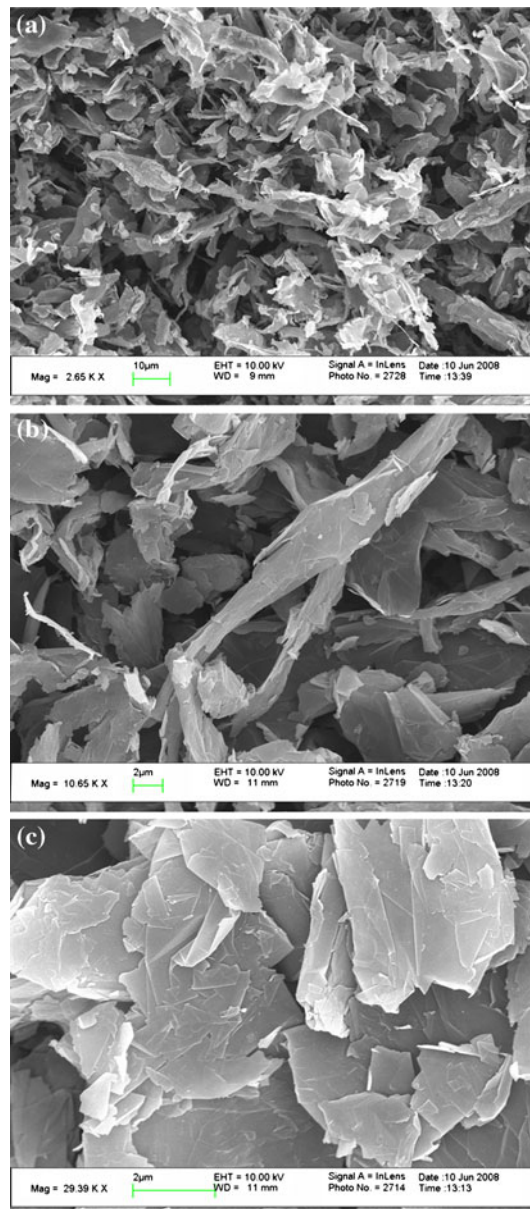


Fig. 1 SEM micrographs of NGP-1 in progressive magnifications where **a** 2.65 kX, **b** 10.65 kX, and **c** 29.39 kX

SEM micrographs of NGP-1 in 2.65, 11, and 29 kX magnifications, respectively. The SEM micrographs show that the NGP-1 materials are in stacks of platelets and their dimensions are about 10 μm in size.

Figure 2a–c shows the SEM micrographs of NGP-2 in progressive magnifications in 2, 10, and 23 kX, respectively. The NGP-1 and NGP-2 are very similar in appearances with the exceptions that the NGP-2 stacks seem thicker than the NGP-1 stacks.

Figure 3a–c shows the SEM micrographs of NGP-3 in progressive magnifications of 3, 12, and 52 kX, respectively. A lot of impurities (white particles) were found on the surfaces of the NGP-3 which were not found on other

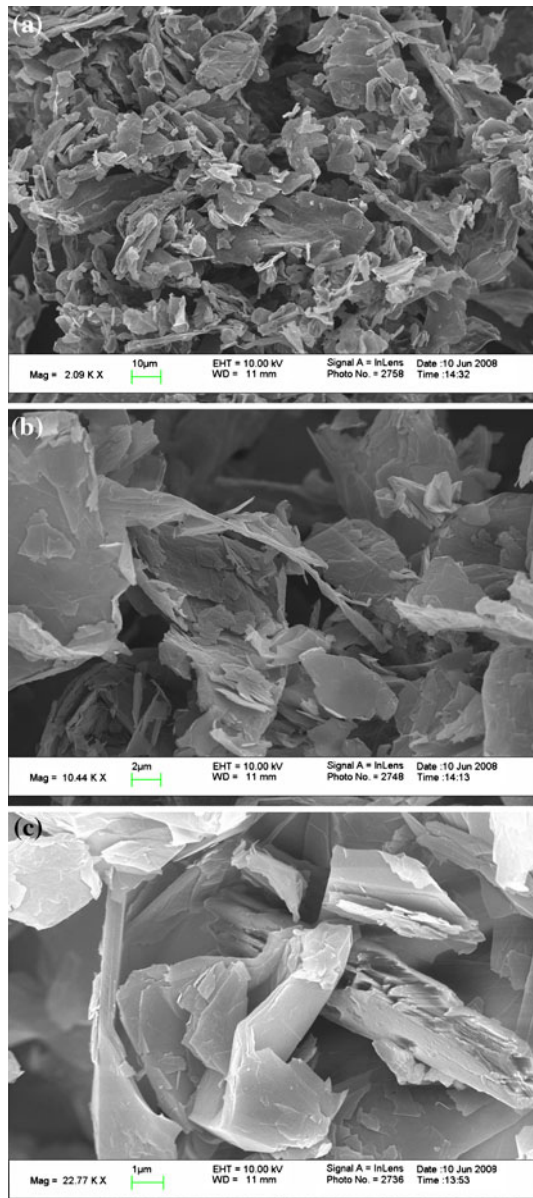


Fig. 2 SEM micrographs of NGP-2 in progressive magnifications where **a** 2.09 kX, **b** 10.44 kX, and **c** 22.77 kX

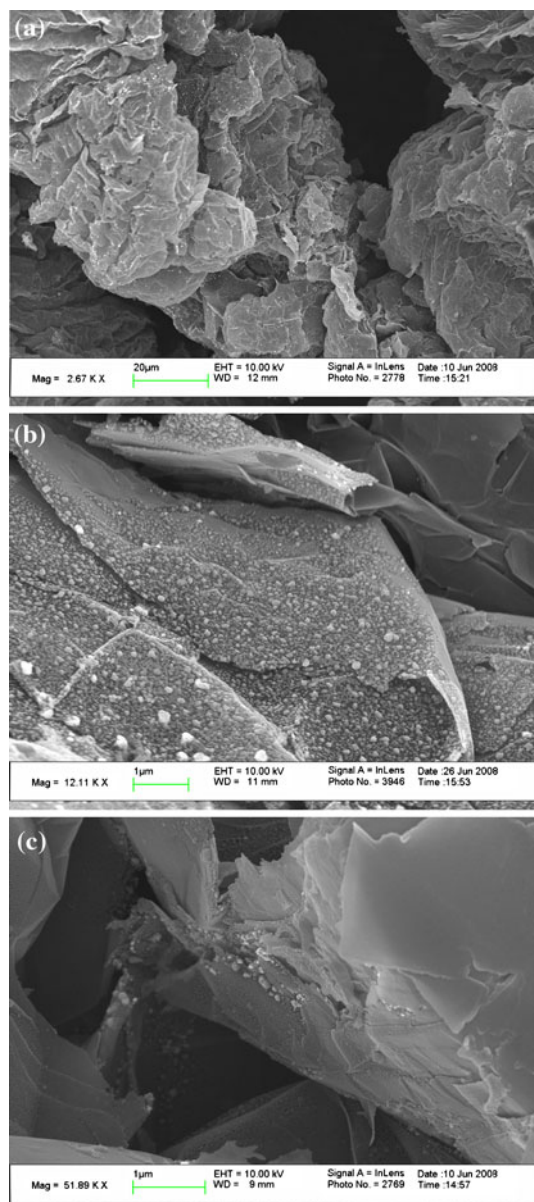


Fig. 3 SEM micrographs of NGP-3 in progressive magnifications where **a** 2.67 kX, **b** 12.11 kX, and **c** 51.99 kX

NGP materials. The dimensions of NGP-3 are in 20 μm size and are larger than other NGP materials used in this study.

Figure 4a–c shows the SEM micrographs of NGP-4 in 2.24, 10, and 23 kX magnifications, respectively. This NGP-4 is larger in size than NGP-1 and NGP-2, but smaller than NGP-3 material.

Thermal stability characterization

Thermogravimetric analysis was conducted on NGP-1, NGP-2, NGP-3, and NGP-4 specimens at heating rates of 5, 20, and 40 °C/min in an Ar atmosphere. We are unable to conduct TGA experiments successfully for the NGP-5 specimen due

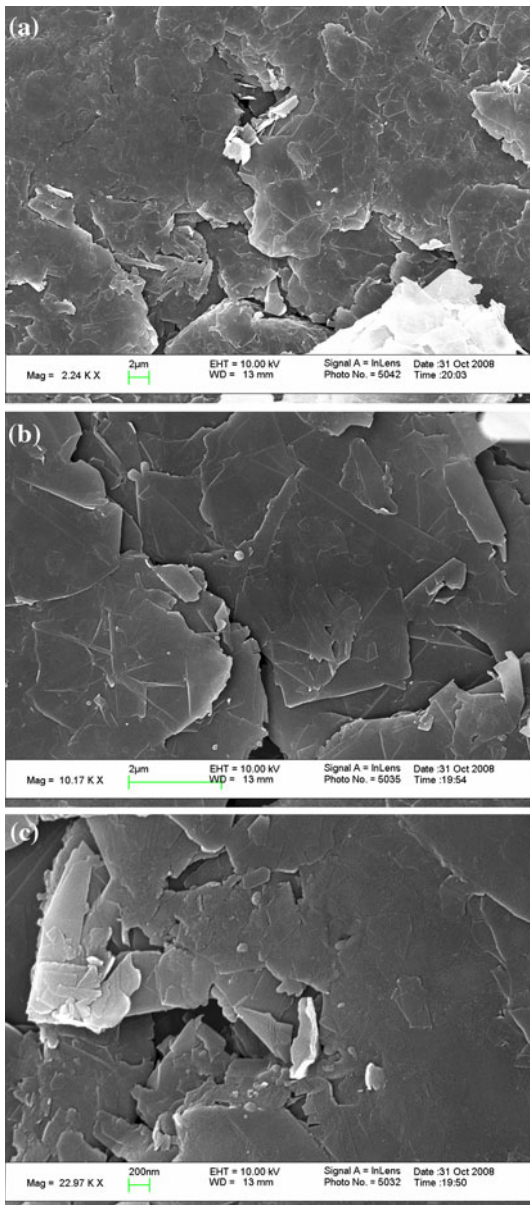


Fig. 4 SEM micrographs of NGP-4 in progressive magnifications where **a** 2.24 kX, **b** 10.17 kX, and **c** 22.97 kX

to the extensive exothermic reaction occurs even in the inert atmosphere. A special experiment is needed to be designed to conduct this experiment successfully. Figure 5 shows a comparison of all NGPs at 5 °C/min in an Ar atmosphere. There are some differences in the thermal stability for these four types of NGPs. At low heating rate (5 °C/min), NGP-1 is the most thermally stable, followed by NGP-2, then NGP-3, and NGP-4 has the least thermal stability. Table 2 shows the residual mass of the four NGPs for the three heating rates. The bold values in Table 2 indicate the largest residual masses at 5, 20, and 40 °C/min heating rates.

Figure 6 shows at medium heating rate (20 °C/min), the most thermally stable material is NGP-2, followed by

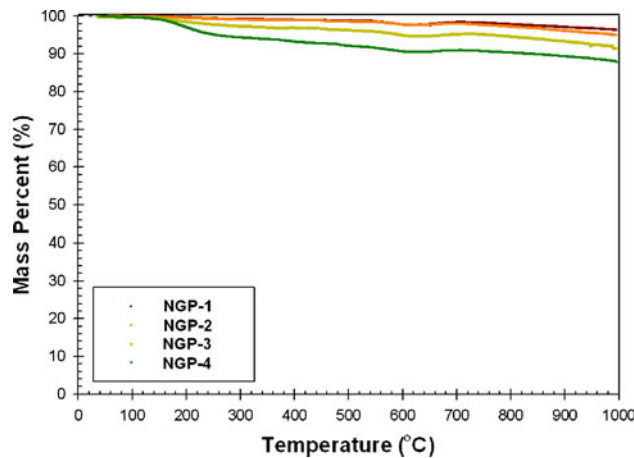


Fig. 5 Comparison of NGPs at heating rate of 5 °C/min in an Ar atmosphere

Table 2 Residual mass of different NGPs for three heating rates in Ar

NGP	Residual mass at 5 °C/min (%)	Residual mass at 20 °C/min (%)	Residual mass at 40 °C/min (%)
NGP-1 (Brazil)	96.3	80.6	49.6
NGP-2 (Graftech)	94.9	87.1	84.0
NGP-3 (Russian)	91.5	76.4	57.2
NGP-4 (XGSciences)	88.0	84.0	62.2

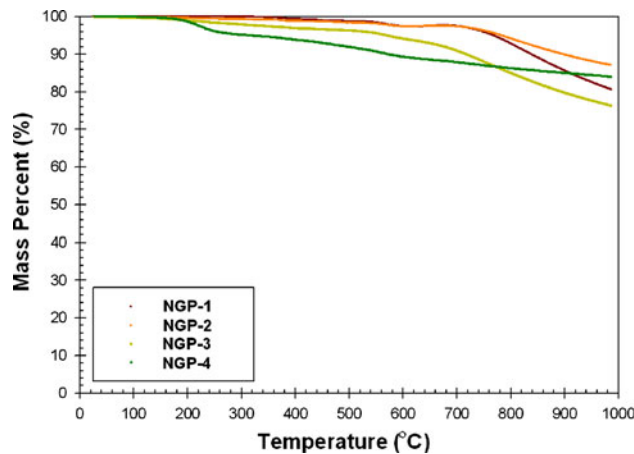


Fig. 6 Comparison of NGPs at heating rate of 20 °C/min in an Ar atmosphere

NGP-4, then NPG-1, and NPG-3 is the least thermally stable material (Table 2).

Figure 7 shows at high heating rate (40 °C/min), the thermal stability of the NGPs is substantially different, NGP-2 with 84% residual mass at 980 °C, NGP-4 with 62% residual mass, NGP-3 with 57% residual mass, and

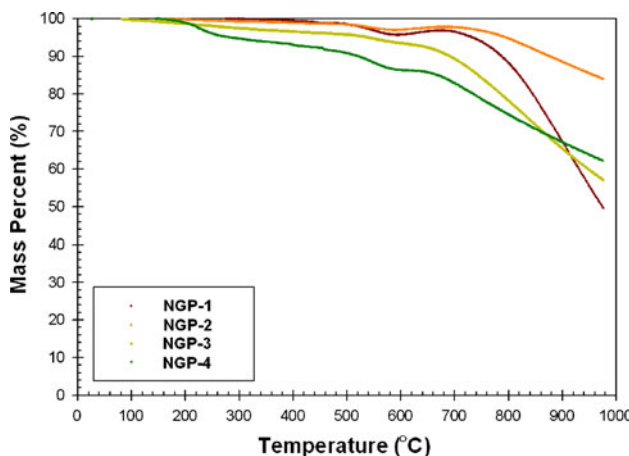


Fig. 7 Comparison of NGPs at heating rate of 40 °C/min in an Ar atmosphere

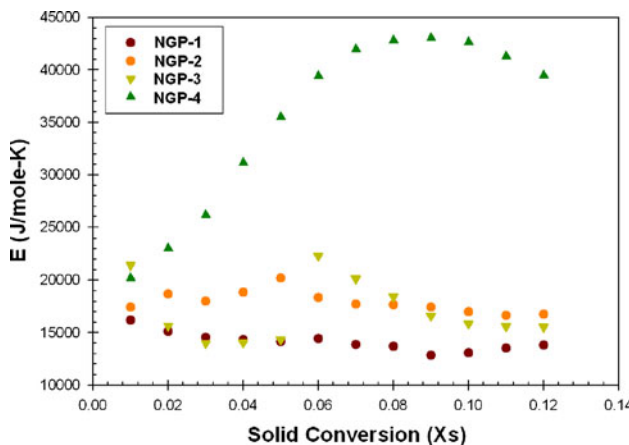


Fig. 8 Activation energy (E) of several NGPs

NGP-1 with 50% residual mass (Table 2). In general, the NGP-2 material is the most thermally stable material, followed by the NGP-4 material in this study. It has shown that NGPs behave very differently under thermal loading. For thermal application, one should choose the more thermally stable NGP.

Kinetics calculation

The activation energies of the different NGPs were calculated using the isoconversion method. Because the isoconversion method gives activation energies dependent on the solid conversion, the averages have been taken in order to meaningfully compare the formulations. Figure 8 shows the activation energies of the four NGPs and Table 3 is a summary of the kinetic parameters of these NGPs. Average (E_{avg}) and peak (E_{peak}) activation energy of NGPs show distinct differences (Table 3). The bold values in Table 3 indicate the NGP-4 has the highest average and peak

Table 3 Kinetic parameters of different NGPs

NGP	E_{avg} (kJ/mol K)	E_{peak} (kJ/mol K)	A_{avg}	Solid conversion range
NGP-1 (Brazil)	15.0	16.15	5.28E01	0.01–0.04
NGP-3 (Russian)	17.5	22.33	4.84E02	0.01–0.08
NGP-2 (Graftech)	18.6	20.17	3.68E02	0.01–0.05
NGP-4 (XGSciences)	35.6	43.04	2.93E04	0.01–0.12

activation energy amongst the four NGPs. Based on E_{avg} , NGP-4 is the best, followed by NGP-2, then NGP-3, and NGP-1 is the worst.

Summary and conclusion

Microstructural analyses were conducted on four NGPs using SEM analyses. NGP-1 and NGP-2 are very similar in size about 10 μm. NGP-3 is the largest in size (>20 μm) amongst these four NGPs.

In general, the NGP-2 material is the most thermally stable material especially under high heating rate (40 °C/min), followed by the NGP-4 material. Under low heating rate, there is no significant difference in thermal stability for all NGPs in this study.

Average and peak activation energy of NGPs show distinct differences. Based on average E (E_{avg}), NGP-4 is the best, followed by NGP-2, then NGP-3, and NGP-1 is the worst.

Based on the above results, two candidate NGPs (NGP-2 and NGP-4) materials were selected for further studies. NGP-4 was blended with polyamide 11 (PA11) powder using the Thinky mixer and acoustic resonance mixer [20, 21]. Cured films of the PA11-NGP materials were pressed to further examine their thermal stability [21] and electrical conductivity [20, 21] properties measurements [20]. Additional material properties such as mechanical and flammability are in progress.

References

1. Pinnavaia TJ, Beall GW (eds) (2000) Polymer-clay nanocomposites. Wiley, New York
2. Koo JH (2006) Polymer nanocomposites: processing, characterization, and applications. McGraw-Hill, New York
3. Morgan AB, Wilkie CA (eds) (2007) Flame retardant polymer nanocomposites. Wiley, Hoboken, NJ
4. Gupta RA, Kennel E, Kim KJ (eds) (2010) Polymer nanocomposites handbook. CRC Press, Boca Raton, FL
5. Mittal V (ed) (2010) Polymer nanotube nanocomposites: synthesis, properties, and applications. Wiley, Hoboken, NJ
6. Mittal V (ed) (2010) Optimization of polymer nanocomposites properties. Wiley-VCH, Weinheim

7. Jang BZ, Zhamu A (2008) *J Mater Sci* 43:5092. doi:[10.1007/s10853-008-2755-2](https://doi.org/10.1007/s10853-008-2755-2)
8. Lao SC, Wu C, Moon TJ, Koo JH, Morgan A, Pilato L, Wissler G (2009) *J Compos Mater* 43:1803
9. Lao SC, Wu C, Moon TJ, Koo JH, Pilato L, Wissler G (2010) *J Compos Mater.* doi:[10.1177/0021998310369580](https://doi.org/10.1177/0021998310369580)
10. Ávila AF, Universidade Federal de Minas Gerais, Department of Mechanical Engineering, Belo Horizonte, Brazil (aavila@netuno.lcc.ufmg.br)
11. Ávila AF (2009) In: Columbus F (ed) Composites performance and trends. Nova Science Publishers, Hauppauge, NY
12. Miller SG (2008) Effects of nanoparticle and matrix interface on nanocomposite properties. Ph.D. dissertation, University of Akron, Akron, OH
13. Schmidt HK, Rice University, Chemical and Biomolecular Engineering Department, Houston, TX (hks@rice.edu)
14. XG Sciences, Inc. at East Lansing, MI (www.xgsciences.com)
15. Ruoff R, Department of Mechanical Engineering, the University of Texas at Austin (r.ruoff@mail.utexas.edu). Abundant technical information can be found in Professor Ruoff's website (www.bucky-central.me.utexas.edu)
16. Rilsan® polyamide 11 technical data sheet, Arkema Inc., France
17. Vestamid® polyamide 12 technical data sheet, Evonik, D-63403, Hanau-Wolfgang, Germany
18. Ceamanos J, Mastral JF, Millera A, Aldea ME (2002) *J Anal Appl Pyrolysis* 65:93
19. Day M, Budgell DR (1992) *Thermochim Acta* 203:465
20. Chen DZ, Lao SC, Koo JH, Londa M, Alabdullatif Z (2010) Powder processing and properties characterization of polyamide 11-graphene nanocomposites for selective laser sintering. In: Proc. 2010 solid freeform fabrication symposium, Austin, TX, August 2–4
21. Jacobs CJ, Tate JS, Olson B, Koo JH (2010) Thermal characterization of polyamide 11/nanographene platelet nanocomposites. *J Nanosci Nanotechnol* (under review)